

Radiation Physics and Engineering 2022; 3(1):39–42

<https://doi.org/10.22034/RPE.2022.336055.1064>

# Calculation of magnetic field effects on dose distribution inside a heterogeneous phantom in MR-guided helium ion-therapy using FLUKA Monte Carlo simulation code

Nahid Hajiloo\*

Radiation Application Research School, Nuclear Science and Technology Research Institute, P.O. Box 31485-498, Karaj, Iran

## HIGHLIGHTS

- The perturbations caused by the presence of a magnetic field in the dose profile delivered to the patient is investigated.
- Tissue heterogeneity can cause significant variation in the boundary of heterogeneous layers.
- Dose changes depends on the location of heterogeneous layers, thickness and the energy of helium ions.

## ABSTRACT

In this work, the impact of magnetic field presence on the central axis depth-dose curves of helium ion beams inside a heterogeneous phantom with air and bone layers was investigated. According to the calculations, presence of the magnetic field has a considerable impact on the dose distribution of helium beams depending on the field strength and beam energy. A 32.3% abrupt increase and 92.5% reduction in dose were observed at the boundary between the water-air and the water-bone layer insert, respectively. The accuracy of the simulation was evaluated by verifying the depth dose curves of helium ion beams in a water phantom with experimental data.

## KEYWORDS

Dosimetry  
Ion-therapy  
Helium ions  
FLUKA Code  
MR-Guided therapy

## HISTORY

Received: 04 April 2022  
Revised: 20 April 2022  
Accepted: 21 April 2022  
Published: Winter 2022

## 1 Introduction

A key challenge in radiotherapy is to maximize radiation doses to cancer cells while minimizing the damage to surrounding healthy tissue. In 1946, for the first time, Wilson proposed to use high-energy ions in radiation therapy (Wilson, 1946). He recommended that specific ionization properties of heavy particles are usable in clinical and biological applications (Schardt et al., 2010; McDonald and Fitzek, 2010). In this type of treatment, the beam range is easily controllable and the beam is delivered with high precision to small defined volumes in the body. For the past decades, hadron therapy using proton, carbon, iron, oxygen and helium particles has been considered, so that by the end of 2015, about 150,000 people have been treated with this method. Currently only carbon ions and protons are being used to treat patients, clinically. Alternative ions such as oxygen and helium are also used in special cases (Sokol et al., 2017). Because of the physical and

radiobiological properties of helium ions compared to the most clinically available ion beams (i. e., proton and carbon), such as beam sharpness and less fragment, currently in the Heidelberg Ion-Beam Therapy (HIT) Center, alongside other ions, the research on the use of helium ions in treatment is conducted (Sokol et al., 2017; Knäusl et al., 2016; Tessonnier et al., 2017a).

Advances in image-guided radiotherapy (IGRT) have allowed for dose escalation and more precise radiation treatment delivery. Each decade brings new imaging technologies to help improving RT patient setup. Currently, the most frequently used method of three-dimensional pre-treatment image verification is performed with cone beam CT. However, more recent developments have provided RT with the ability to have on-board MRI coupled to the radiotherapy unit. This latest tool for treating cancer is known as MR-guided RT. Varieties of these units have been designed and installed in centers across the globe. MR-gRT has an array of advantages over traditional types

\*Corresponding author: [nhajiloo@aeoi.org.ir](mailto:nhajiloo@aeoi.org.ir)

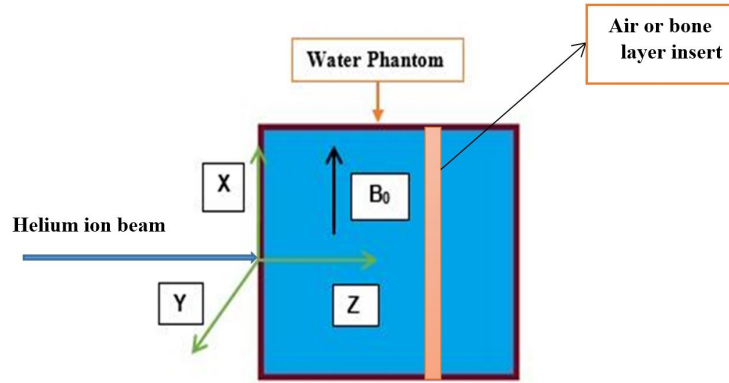


**Figure 1:** Homogeneous phantom consisting of a 3-cm thick heterogeneous layer of air or bone insert. The location of the air and bone layers was ranging 25 to 28 cm in depth.

of IGRT platforms, but it does have some limitations that must be addressed. Although attempts have been made to create a suitable shield for the magnetic field around the MRI systems, the magnetic field of the MRI system has an effect on the particle accelerator, which is not negligible, especially in the patient's position, and its presence causes changes in dose distribution. By investigation of these changes and accurately estimating them, changes in dose distribution can be compensated in some way. In order to identify such effects, in this study, using the Monte Carlo FLUKA code, the changes in the dose distribution of helium ions beam, used in a heterogeneous phantom, including water, bone and air in the presence of a uniform magnetic field, were estimated.

## 2 Materials and method

If a charged particle of mass  $m$  and charge  $q$  is placed in a constant magnetic field ( $B_0$ ), according to Eq. (1), a force is applied to the charged particle by the magnetic field, the amount of which depends on the amount of charge and velocity of the particle as well as the magnetic field strength (Change, 2016). Therefore, it is expected that when helium ions are exposed to a magnetic field, a magnetic force will be applied to them and changes in the dose distribution will occur.

$$F = qV \times B_0 \quad (1)$$

In this research, FLUKA Monte Carlo code (version 2011.2c.5) has been used for simulation (Ferrari et al., 2005). In order to compare the available experimental data with the results of the calculations, a mono-energy, single-directional therapeutic beam was simulated and the spatial distribution of the particles was considered with a rectangular distribution dimensions of 6.3 mm. Also, some important cards that were utilized in this work, accompanied by a short description, were shown in Table 1. The energies of the beams were supposed to be 56.4, 79.8, 103.1, 122.9, 140.7, 157, 172.3, 190.9, 210.9, and 220.5 MeV.n<sup>-1</sup> (Table 2). Since the experimental data for beam simulation validation was available in the literature only for the studied energies, these energies were selected.

A water phantom with dimensions of  $30 \times 30 \times 30$  (in cm<sup>3</sup>) was simulated. Due to the existence of experimental data in the studied energies without the presence of a magnetic field, these energies were selected for the case of the magnetic field influence. The magnetic field perpendicular to the direction of the beam along the +X axis was simulated inside the phantom.

The accuracy of the simulation was evaluated by verifying the depth-dose curves of helium ion beams in a water phantom with experimental data without the magnetic field influence (Tessonier et al., 2017b; Sommerer et al., 2006; Ferrari et al., 2005). Moreover, to achieve a statistical error of less than 1% in the Monte Carlo simulation, minimum and maximum histories of  $4.5 \times 10^6$  and  $10^8$  particles were considered depending on particle energy studied in this article.

The impact of the magnetic field presence on the central axis depth-dose curves inside a heterogeneous phantom (see Fig. 1) with 3 cm thick air and bone layers was investigated. The location of the air and bone layers was ranging from 25 to 28 cm in depth. Bone and air densities were considered to be 1.85 and 0.001 g.cm<sup>-3</sup>, respectively. The incident helium beam energy and the magnetic field studied in this scenario were 250 MeV.n<sup>-1</sup> and 3.0 T, respectively.

The bin size was considered to be 1 mm in the non-Bragg region and 0.25 mm in the Bragg area. To achieve a relative error of less than one percent in dose calculation,  $10^8$  particles were simulated.

## 3 Results

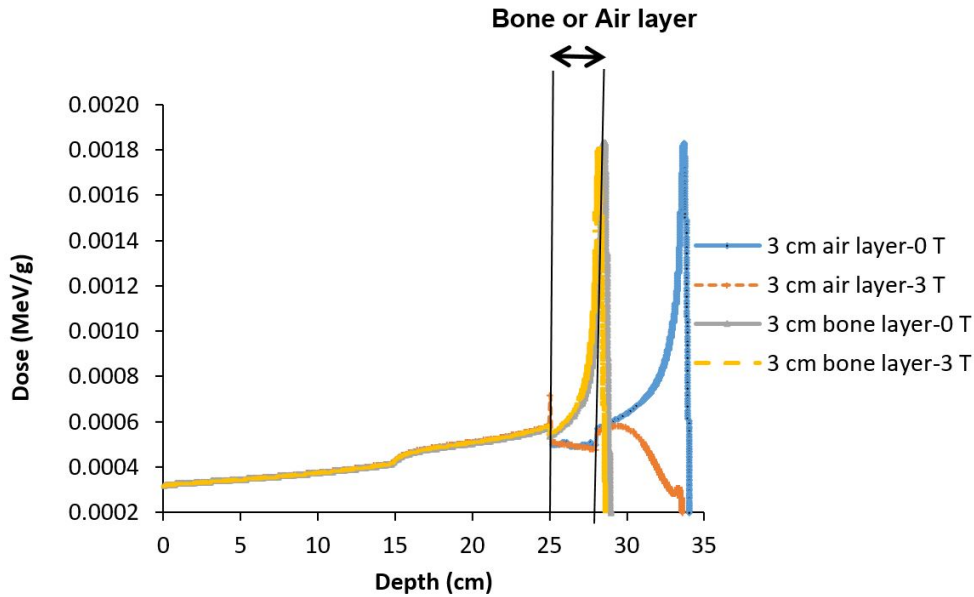
Figure 2 shows the one-dimensional depth-dose distribution of helium ion beams with the energy of 220.5 MeV.n<sup>-1</sup> inside a heterogeneous phantom with 3-cm thick layers of bone and air. In the presence of an air layer inside the phantom, as can be seen in Fig. 2, at the boundary between water and air, an increase in dose occurs due to the Electron Return Effect (ERE) phenomenon (Raaymakers et al., 2008) in which the deflection of the secondary electrons in backward direction leads to an overdose of the first layer between two interfaces. The reason for the im-

**Table 1:** FLUKA code cards that were utilized in this study (Ferrari et al., 2005).

Card name	Description
Defaults	Set the code defaults for a specific type of problem.
MGN field	Set the particle tracking conditions for transportation in the presence of magnetic fields.
USRBIN	Set the distributions of physical values in a regular spatial structure, which does not depend on the geometry.
BEAM	Define primary beam characteristics.
STEPSIZE	Set the Particle step sizes on a region-by-region basis.

**Table 2:** Comparison of the Bragg peak depth values of the helium ion beams calculated in this study with the experimental values published in the literature (Tessonnier et al., 2017b).

$E$ (MeV.n <sup>-1</sup> )	Experiment (Tessonnier et al., 2017b)	Simulation FLUCA (This work)	Discrepancy (%)
56.4	27.5	27.67	0.17
79.8	52.0	51.59	-0.41
103.1	81.5	81.46	-0.04
122.9	112.0	111.20	-0.80
140.7	142.0	141.04	-0.96
157	171.5	170.84	-0.66
172.3	201.0	200.88	-0.12
190.9	240.5	239.61	-0.89
210.9	285.0	284.24	-0.76
220.5	307.5	306.64	-0.86

**Figure 2:** One-dimensional depth-dose distribution of helium ion beams with the energy of 220.5 MeV/n inside a heterogeneous phantom containing bone or air layer.

portant changes at the depth-dose in the presence of a magnetic field and the heterogeneity of the air is the increase in the deflection of the helium beam inside the air layer, which leads to a sharp decrease in the dose profile at the Bragg peak. In the presence of a bone layer, an important impact on the depth-dose curve compared to the case without a magnetic field was observed.

To better display the dose changes in the central axis direction in the presence of the 3.0 T magnetic field applied to heterogeneous phantoms, including the air and bone layers, the percentage of dose changes in the direc-

tion of the central axis after applying the field is displayed in Fig. 3. The formula for calculating dose difference is as follows (Eq. (2)):

$$Dose\ reduction\ (\%) = \frac{D_{3.0T} - D_{0.0T}}{D_{0.0T}} \times 100 \quad (2)$$

In this equation,  $D_{0.0T}$  and  $D_{3.0T}$  are the dose in the presence of 0.0 and 3.0 T fields, respectively.

In the presence of the air layer, a 32.3% abrupt increase in dose due to magnetic field application at the boundary between the water and air, which is due to the ERE phenomenon. In the presence of the bone layer, a

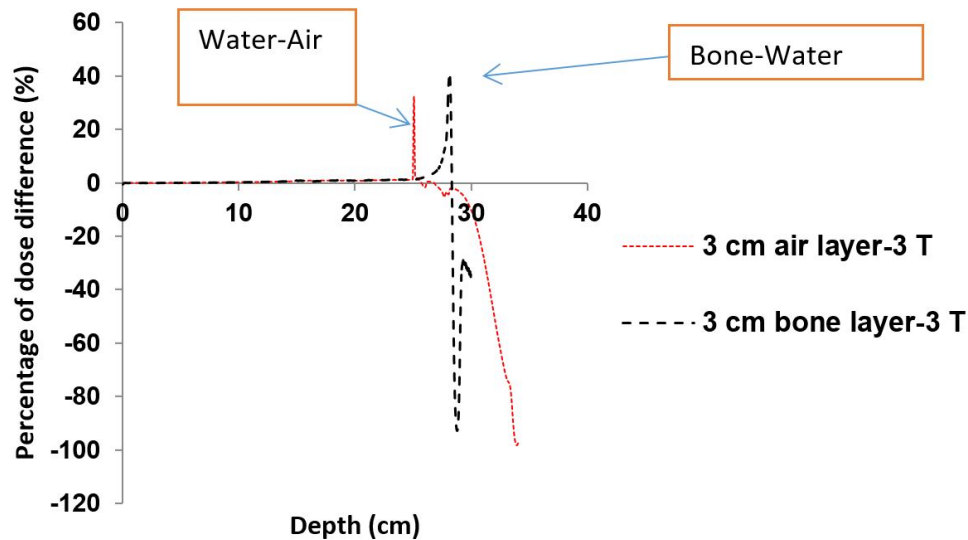


**Figure 3:** Percentage of dose changes along the central axis after applying a 3.0 T magnetic field inside heterogeneous phantoms, including air or bone layers.

92.5% reduction in dose occurs compared to the absence of a field at the boundary between bone and water.

## 4 Conclusion

The presence of heterogeneous layers of air and bone leads to a considerable variation in the boundary of these layers with water due to the presence of a magnetic field. The amount of dose changes might depend on the location of these inhomogeneous layers relative to the Bragg depth, thickness, and the energy of the incident beam. A 32.3% abrupt increase and 92.5% reduction in dose were observed at the boundary between the water-air and the water-bone layer insert, respectively.

## References

- Change, D. (2016). *Field and wave electromagnetics, second edition*. Syracuse University.
- Ferrari, A., Ranft, J., Sala, P. R., et al. (2005). *FLUKA: A multi-particle transport code (Program version 2005)*. Number CERN-2005-10. Cern.
- Knäusl, B., Fuchs, H., Dieckmann, K., et al. (2016). Can particle beam therapy be improved using helium ions?—a planning study focusing on pediatric patients. *Acta Oncologica*, 55(6):751–759.
- McDonald, M. W. and Fitzek, M. M. (2010). Proton therapy. *Current Problems in Cancer*, 34(4):257–296.
- Raaymakers, B. W., Raaijmakers, A. J., and Lagendijk, J. J. (2008). Feasibility of MRI guided proton therapy: magnetic field dose effects. *Physics in Medicine & Biology*, 53(20):5615.
- Schardt, D., Elsässer, T., and Schulz-Ertner, D. (2010). Heavy-ion tumor therapy: Physical and radiobiological benefits. *Reviews of Modern Physics*, 82(1):383.
- Sokol, O., Scifoni, E., Tinganelli, W., et al. (2017). Oxygen beams for therapy: advanced biological treatment planning and experimental verification. *Physics in Medicine & Biology*, 62(19):7798.
- Sommerer, F., Parodi, K., Ferrari, A., et al. (2006). Investigating the accuracy of the FLUKA code for transport of therapeutic ion beams in matter. *Physics in Medicine & Biology*, 51(17):4385.
- Tessonnier, T., Mairani, A., Brons, S., et al. (2017a). Experimental dosimetric comparison of  $^1\text{H}$ ,  $^4\text{He}$ ,  $^{12}\text{C}$  and  $^{16}\text{O}$  scanned ion beams. *Physics in Medicine & Biology*, 62(10):3958.
- Tessonnier, T., Mairani, A., Brons, S., et al. (2017b). Helium ions at the heidelberg ion beam therapy center: comparisons between FLUKA Monte Carlo code predictions and dosimetric measurements. *Physics in Medicine & Biology*, 62(16):6784.
- Wilson, R. R. (1946). Radiological use of fast protons. *Radiology*, 47(5):487–491.